

CS-31
R. Yamada
S. Mori
April 27, 1966

MAGNETIC FIELD MEASUREMENT I

Introduction

The Cornell 10 GeV alternating-gradient electron synchrotron, with a diameter of 100m is among the largest synchrotrons existing or under construction. Accordingly, the stability region is very small and high accuracy is required for the pole profile of magnets. Gap heights are one and one-half inches for a wide gap magnet (vertical focusing: positive) and about one inch for a narrow gap magnet (radial focusing: negative). These are the smallest gaps of all synchrotrons. Therefore, the accuracy needed for stamping laminations of the magnets is the most stringent. They were made with an accuracy of ± 0.25 mil. Gradients in the usable region are required to be within a limit of about $\pm 0.5\%$ from the designed values. ¹⁾

Measurement of magnetic field must be carried out with a comparable accuracy with the above requirement. We have measured the absolute value of $X_0 (=B_0 / (\frac{dB}{dx})_0)$ with an accuracy of $\pm 0.15\%$ and the distribution of $X_0(x)$ with a relative accuracy of $\pm 0.1\%$. The measurement was done with high AC excitation of the magnet without and with a DC bias, using search coils and an integrator. The magnetic field at the center was from 2.5 to 5kG (the peak field at an excitation of 15 GeV), which is free from the remanent field and the saturation effect.

The actual profile of pole pieces were determined through computer calculation which assumed a constant magnetic length of 127.5" and a constant gradient length of 126.5", while a

geometrical length of the lamination stack is 126.48" for two types of magnets. 1, 2)

Eringing fields at the ends of the magnets were measured at high AC field using the same technique. Effective magnetic and gradient lengths were also measured along the radial direction. Several hard packs (groups of laminations with a graded profile which are prefabricated for use at the ends of magnets), which were different in shape, were made and measured in order to obtain designed constant magnetic and gradient lengths in the usable regions at high field.

Excitation Curve

The magnet is excited with a DC power supply and the field in the gap was measured with a Rawson rotating coil fluxmeter. The excitation curves of the narrow gap magnet at the center and at one inch outside are shown in Fig. 1. The saturation starts around 16 GeV, but it is due to the thinner back legs, which are 1-1/4" on both sides compared to 4" of the pole piece width. Therefore the gradient of the field is probably not seriously affected by saturation for both types of magnets at least up to 20 GeV. A similar curve was obtained for the wide gap magnet.

Absolute Value of X_0 at the Center

The X_0 at the center was measured with two small search coils and an integrator. 3) One of the search coils was fixed at some point in the gap as a standard coil and the other moving coil was set at the center at first. A schematic diagram of the system is shown in Fig. 2. The output voltage of the moving coil was compared with that of the standard coil by using voltage dividers. The polarities of the two search coils were opposite so that they were bucking each other. The output of the search coils connected in series was fed into an integrator and then into an oscilloscope,

which was triggered by the signal from a peaking strip placed in the gap. The divider for the standard coil was adjusted such that voltage levels at the two points, where the magnetic field was zero and the maximum, became equal on the scope.

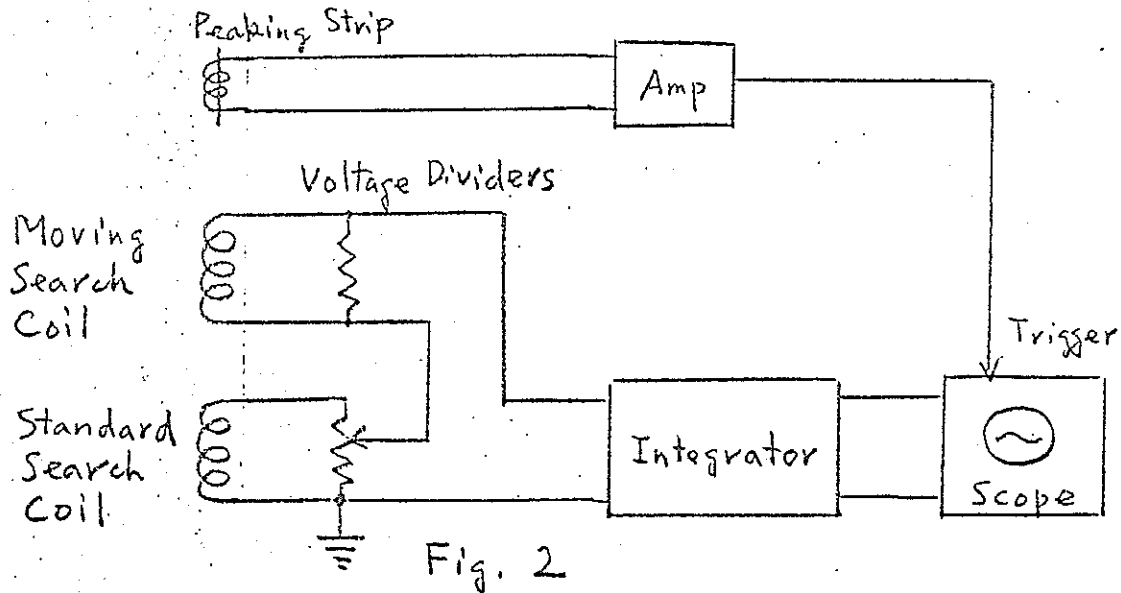


Fig. 2

The output voltage V_o of the two coils connected in series is given by

$$V_o = V_m \frac{R_d}{R_d + R_c} - \alpha V_s \frac{R_d}{R_d + R'_c}, \quad (1)$$

where V_m and V_s are the output voltages of the moving and standard coils, respectively, α is the setting of the divider for the standard coil, and R_d , R_c and R'_c are the impedances of each divider, the moving coil and standard coil, respectively. The two coils were made identical and $R_c = R'_c = 34 \Omega$, and $R_d = 10 \text{ k}\Omega$. Then the output of the integrator V at $t = t_1$ is given by

$$V = \int_{t_0}^{t_1} V_o dt = \frac{R_d}{R_d + R_c} \frac{1}{RC} \int_{t_0}^{t_1} (V_m - \alpha V_s) dt, \quad (2)$$

where R and C are the input resistor and the feedback capacitor of the integrator, respectively. V_m and V_s are expressed as

$$V_m = A_m \cdot \frac{dB_m}{dt}, \text{ and } V_s = A_s \cdot \frac{dB_s}{dt}, \quad (3)$$

where A_m and A_s are the turn areas of the moving and standard coils, and B_m and B_s are the magnetic fields at the positions where the moving and standard coils are located, respectively. The two coils are almost identical, and $A_s = \beta A_m$, where β is nearly equal to one. Then Eq(2) can be rewritten as

$$V = \frac{R_d}{R_d + R_c} \cdot \frac{A_m}{RC} \left[B_m - \alpha \beta B_s \right]_{t_0}^{t_1} \quad (4)$$

B_m and B_s at t_0 are less than a few gauss and their difference is much smaller than the values at t_1 , and we adjust the divider to make $V=0$ on the scope. Therefore

$$B_m(t_1) = \alpha \beta B_s(t_1). \quad (5)$$

Since $\beta B_s(t_1)$ is constant, α gives the relative field intensity at the moving coil at $t=t_1$.

First the central field was measured as mentioned above and the moving search coil was moved in x direction for a given distance (usually $\pm 0.5''$) and the fields at these points were measured also with respect to the standard coil. We took their difference ΔB . $X_0(0)$ is then given by

$$X_0(0) = \frac{B_0(0)}{\left(\frac{\Delta B}{\Delta X} \right)_0} \quad (6)$$

General Radio 1454-A Decade Voltage Dividers were used, which have a maximum linearity error of $\pm 0.02\%$ and a frequency error of less than 0.1% up to 20kc. They are four digit dividers. We added a 0.1 Ω -10 step variable resistor in series with the dividers to read out another digit. Sometimes we used the deflection on the scope for reading out the fifth digit.

The integrator used was Tektronix "0-type" plug-in which was set at the input impedance of 100k Ω and feedback impedance of 0.01 μ F. Its open gain is 2000 and the effective time constant was 2 sec. which was good enough for the measurement of 60 c/s AC field measurement. There was a small error of about 0.1% in the integration due to the finite gain of the integrator. But this results in a negligible error because only a very small difference signal is integrated. A Tektronix RM 561A - oscilloscope with a 2A63 plug-in unit was used for the display and adjustment of level of the output signal. The sensitivity of the scope was set at ~ 2 mV/cm.

A peaking strip was used to trigger this scope. The delay of its signal (a few μ s) and the effect of the remanent field (3-4 gauss) were small compared to the peak field. So, in our present measurement it can be neglected as we were interested only in the field shape due to the pole profile.

The main error of the measurement of $X_0(0)$ came from uncertainty in the positioning of the moving coil at the center of the pole piece gap. This was estimated to be ± 7 mils. Since the field gradient is about 11% / inch, an uncertainty of 0.08% is estimated in the central field value and in $X_0(0)$ due to this effect.

The positioning of the moving coil was done by an indirect method as we could not measure directly the position of the coil far inside the gap. In this indirect method the level of the

magnet was set and the axis of a transit was aligned on the center line of the magnet by using special jigs. A mill table which carried the coil was leveled and aligned parallel to the axis of the magnet by using a micro-dial gauge on the mill table and a long parallel bar extending from one side of the magnet. The search coil, which had a sharp cone as a center pointer, was placed on the center line of the magnet outside the gap with the aid of the transit. Then the search coil was moved about one foot into the gap, where the central field was measured. There might have been a small error due to the inclination and the imperfection of the search coil (< 2 mils).

We measured the radial displacement Δx with a dial gauge and gauge blocks. The possible error in Δx is estimated to be less than 0.5 mil for 1.000" displacement, i.e. 0.05%. Uncertainty in ΔB , which was taken as a difference between two five-digit numbers ($\sim 10^5$), was about 0.02% (corresponding to four-digits) since $\Delta B/B$ was about 0.1. The $X_0(x)$ is not a constant throughout the usable region as will be shown later, but has a linear term of a sextapole. The error in $X_0(0)$ due to the finite values of ΔB and ΔX is negligible for the constant field gradient modified with a linear term. If there had been any big higher terms, the exact value of $X_0(0)$ should be corrected from the curve of X_0 around the center.

The two search coils were made identical with ratios of the diameter to height of 0.72 to give the average central field. The inductance of the coil was about 0.2mH. This is quite small compared to the input impedance of the dividers of 10k Ω . Therefore, its effect was neglected. As two search coils were connected in the opposition any fluctuation in the power supply did make no error.

Thus, the overall uncertainty is estimated to be $\pm 0.15\%$. Table I gives the measured results together with the designed values for both magnets. There was no detectable difference between the values of excitation corresponding to 7.5 and 15 GeV excitation levels.

Table I: Absolute Values of X_0 at the Geometric Center at High Field

Magnet	Gap Height	Designed Value	Measured Value	Measured Minus Designed	Effect of Punching Error
Low Gap	1.022"	9.010"	9.045" \pm 0.014"	+0.035	+0.035"
High Gap	1.501"	9.223"	9.204" \pm 0.014"	-0.019	-0.004"

The errors in the profiles of the punched laminations were measured geometrically. Their effect on $X_0(o)$ were estimated according to Eq. (15) and shown also in Table I. They account for some of the differences between the measured values and the designed ones.

In our case the iron was not saturated so that measurements made without integration gave the same result within the experimental error. Another alternate method was to use two integrators for two search coils and compare them with the dividers. This gave the same results.

Measurement of the Radial Distribution of $X_0(x)$.

We could measure the radial distribution of $X_0(x)$ by the same method as used for the measurement of the absolute X_0 at the center. However, the percentage error was bigger in this case, because the absolute value of Δx was quite small (0.1" \sim 0.2")

and the error in Δx was the same as in the previous case. The precision of the mechanical positioning device was not sufficient to yield an accuracy of better than $\pm 0.5\%$ with this method.

Instead of using a single coil as a moving coil we used matched twin coils consisting of a pair of identical coils glued together. Since the distance between the two coils was kept constant, the error in the Δx was negligible. They were connected in series and bucking each other. The radial distribution of $X_0(x)$ was obtained by moving these twin coils along the radial direction, and by comparing their output with that of another fixed standard coil just as in the case of the absolute X_0 measurement.

The output of the twin coils V_t is given by

$$V_t = A \frac{d}{dt} (B_1 - B_2) = A \frac{d}{dt} (\Delta B), \quad (7)$$

where B_1 and B_2 are the magnetic fields at the centers of the first and second coil of the twin coils and A is the turn area of each coil. V_t and ΔB correspond to V_m and B_m in Eq.(3), respectively. Therefore, the distribution of $\Delta B(x)$ can be obtained by adjusting the divider for the standard coil, and that of $X_0(x)$ being calculated.

Although the geometrical shape and the turn number was made the same for each of the twin coils, there was some difference between them. Therefore an additional single turn on one of the coils was adjusted in area, so that the turn areas of the two coils

were matched. The turn areas of the two coils are A at the magnetic field B and A+ΔA at B+ΔB. Then the output voltage of the twin coil is proportional to

$$(A+\Delta A) \cdot (B+\Delta B) - A \cdot B = A \cdot \Delta B + \Delta A \cdot B + \Delta A \cdot \Delta B. \quad (8)$$

The first term on the right is the term we want and the remaining terms are errors due to the mismatching of the coils. The third term is negligible. The ratio of the error to signal is

$$\left(\frac{\Delta A}{A}\right) \cdot \left(\frac{B}{\Delta B}\right) = 36 \left(\frac{\Delta A}{A}\right). \quad \left(\because \frac{B}{\Delta B} = \frac{X_0}{\Delta X} = \frac{9''}{0.25''} = 36\right)$$

To make the ratio less than 1%, ΔA/A should be made less than 1/3600. Therefore, careful matching of the twin coil is needed. We made ΔA/A less than 1/10000. Since we did not have a homogeneous AC field, the turn-area was adjusted in a constant gradient AC field, by equalizing the outputs obtained by reversing the twin coil

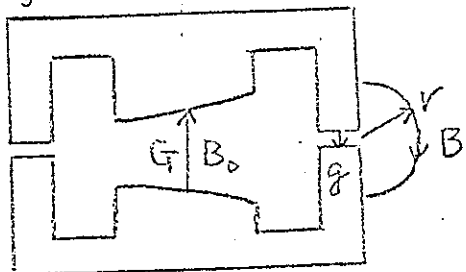
When we take the average of two readings obtained with reverse position of the twin coils, the above second term ΔA·B is cancelled out and the ratio of error to signal is ΔA/2A, which is ~5 X 10⁻⁵

The obtained distributions of X₀(x) for the wide gap and narrow gap magnets are shown in Fig. 3 and Fig. 4. The designed distributions and the ideal lines are shown also in Figs. 3 and 4 with the limit lines of ±0.5%. The agreement between the designed distributions and the measured ones seem fairly good. The measured distributions were same at 7.5 and 15 Gev.

The twin coils used had a spacing of 0.25". Therefore this measurement has a spatial resolution due to the spacing of the twin coils, i.e. 0.25". Therefore the usable region of the actual distribution may be wider on both ends by as much as half this spacing. The widths of the usable regions are estimated 2.35" and 2.75" for the wide gap and the narrow gap magnets respectively including

Measurement of Gap in Back Leg

The magnet is made of top and bottom halves, which are glued together with Epoxy at the centers of the back legs. This gap height g can be measured magnetically using a Hall probe.



It is given by

$$g = \frac{\pi r B}{k B_0} \quad (9)$$

where B_0 is the field at the center of the main gap, kB_0 the field in the gap of the back leg, k is determined by the ratio of the width of the legs and pole piece and by the leakage flux ratio ($k = 1.92$). B is the field at the distance r from the gap of back leg.

Effect of Gap in Back Leg

The calculation of the profile of the pole piece was done assuming a 1 mil gap in the back leg. The measured gap is about 2.0 ± 0.5 mil. And the gap may locally be as large as 3.5 mils. Variation in the back leg gap changes the field distribution, and also moves the isomagnetic line.

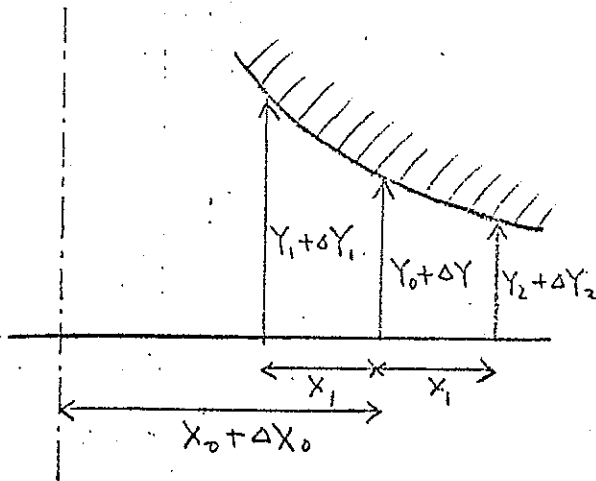
When we have an extra gap Δg on both of the back legs, we have also an extra gap Δg in the central field of the pole piece. Therefore, the change of the field value ΔB_0 at the central field B_0 is,

$$\frac{\Delta B_0}{B_0} = -(1+k) \frac{\Delta g}{G} \quad (10)$$

where G is the gap of the magnet. For 1 mil of Δg , the percentage change in B_0 is 0.3% and 0.2% for 1" gap and 1.5" gap respectively. This change in the field value moves the isomagnetic line by an amount Δx given by

$$\Delta x = -(1+k) X_0 \frac{\Delta g}{G} \quad (11)$$

The amount of shifting due to a 1 mil extra gap is 26 mils and 18 mils for the narrow gap and wide gap magnet respectively.



The approximate amount of change ΔX_0 in X_0 due to an extra gap in the back leg can be derived as follows: Here we treat the case of the constant gradient. The height of the gap from the median plane at the center is Y_0 , and the gaps at X_1 inches away from the center on both sides are Y_1 and Y_2 , Y_1 being taken at the lower field side,

$$X_0 = X_1 \frac{Y_1 + Y_2}{Y_1 - Y_2} \quad (12)$$

If we have error ΔY_1 and ΔY_2 then for the small value of x_1 the total change ΔX_0 is,

$$\Delta X_0 = \frac{X_1}{Y_1 - Y_2} \left\{ (\Delta Y_1 + \Delta Y_2) - \frac{X_0}{X_1} (\Delta Y_1 - \Delta Y_2) \right\} \quad (13)$$

And $Y_1 + Y_2$ is about equal to gap G , then

$$\frac{\Delta X_0}{X_0} = \frac{1}{G} \left\{ (\Delta Y_1 + \Delta Y_2) - \frac{X_0}{X_1} (\Delta Y_1 - \Delta Y_2) \right\} \quad (14)$$

The term $(\Delta Y_1 + \Delta Y_2)$ gives the effect of an extra gap and the term $(\Delta Y_1 - \Delta Y_2)$ the effect due to the inclination of the pole pieces.

If there is an extra gap δ (mil) at the pole pieces and the pole pieces are inclined by e (mil/inch) (e is positive for a bigger gap on the low field side), then

- 12 -

$$\Delta x_0 = 8.8 (\delta - 18\epsilon) \text{ mil, for a narrow gap magnet} \quad (15)$$

$$\Delta x_0 = 6.1 (\delta - 18\epsilon) \text{ mil, for a wide gap magnet}$$

Therefore 1 mil extra gap or 0.05 mil/inch inclination gives of the order of 5~10 mil change, which is about 0.1% of x_0 . These equations can be used for estimation of the accuracy of the lamination profile.

Magnetic and Gradient Lengths

The magnetic length of the magnet at x , $L_B(x)$, is defined by:

$$L_B(x) = \int_{-\infty}^{\infty} B(x, z) dz / B_0(x), \quad (16)$$

where $B_0(x)$ is the magnetic field far inside the magnet at x and z is the coordinate taken in parallel to the magnet axis. Similarly, the gradient length $L_G(x)$ is expressed as

$$L_G(x) = \int_{-\infty}^{\infty} \frac{\partial B(x, z)}{\partial x} dz / \left(\frac{\partial B(x)}{\partial x} \right)_0, \quad (17)$$

where $\left(\frac{\partial B(x)}{\partial x} \right)_0$ is the field gradient far inside the magnet. $L_B(x)$ and $L_G(x)$ refer to the whole magnet with two hard packs (properly shaped prefabricated end sections), and we define $L_B'(x)$ and $L_G'(x)$ for half the magnet with one hard pack. The geometrical length L_{G0} of both magnets i.e. the length of the stacked lamination, is the same and 126.48". The difference between the $L_B'(x)$ and half the L_{G0} is defined as $\Delta L_B'(x)$ and similarly $\Delta L_G'(x)$ is defined for $L_G'(x)$. Therefore,

$$L_B(x) = 2 L_B'(x) = L_{G0} + 2 \Delta L_B'(x), \quad (18)$$

$$L_G(x) = 2 L_G'(x) = L_{G0} + 2 \Delta L_G'(x).$$

The calculation of the operating point and the profiles of the pole pieces was done assuming a constant magnetic length and a constant gradient length for both types of magnets. A half of the

difference between the magnetic and gradient length was assumed half an inch. Therefore, we had to shape the hard packs to satisfy the above requirements. A relation between $L'_G(x)$ and $L'_B(x)$ is given by

$$\begin{aligned} L'_G(x) - L'_B(x) &= \frac{B_0(x)}{\left(\frac{\partial B(x)}{\partial x}\right)_0} \frac{\partial L'_B(x)}{\partial x} \\ &= X_0 \frac{\partial L'_B(x)}{\partial x} \frac{1 + \frac{x}{X_0} + \frac{\epsilon}{2X_0} x^2}{1 + \epsilon x} \\ &= X_0 \frac{\partial L'_B(x)}{\partial x} \left(1 + \frac{x}{X_0}\right) \end{aligned} \quad (19)$$

where X_0 is taken as $(B_0(0) / \frac{\partial B_0(0)}{\partial x})_0$, and ϵ corresponds to a sextapole term inside the gap for the correction of momentum shift of the operating point and it is less than $2.5 \times 10^{-2}/\text{inch}^1$.
At $x=0$, Eq. (19) gives

$$L'_G(0) - L'_B(0) = X_0 \frac{\partial L'_B(0)}{\partial x} \quad (20)$$

As we should make $L'_G - L'_B = -0.5"$, $\frac{\partial L'_B(0)}{\partial x}$ should be made about $\pm 55 \text{ mil/inch}$, where + corresponds to the wide gap and - to the narrow gap magnets.

For beam dynamics the magnetic and gradient lengths are important. Therefore, to make the effect of variation of these lengths negligible, the variations of $\Delta L'_B(x)$ and $\Delta L'_G(x)$ should be made less than $\pm 0.5\%$ of a half of the geometrical length; i.e. less than $\pm 0.3 \text{ inch}$ as $\pm 0.5\%$ was taken as the criterion for the limit of X_0^1 .

Hard Packs and Fringing Field

In order to obtain the final hard packs which satisfied the above requirements, a number of differently shaped hard packs were

tried with successive improvements for both types of magnets. A 10" long search coil with good parallel surfaces was used (10" x 0.4" glass bobbin with 40 turns) for the measurement of the magnetic and gradient lengths. The output of this search coil was compared with another fixed standard as in the case of the $X_0(x)$ measurement.

We set the moving search coil parallel to the z -axis so that it covered from 3" inside to 7" outside with reference to the lamination end, thus, measuring $\int_{-7}^{3} B(x, z) dz$. The origin of z -axis is at the lamination end and it is positive to the inside. Then we measured $\int_{-6}^{4} B(x, z) dz$ by moving the coil one inch into the magnet. As we can see later $z = +3''$ is well inside the uniform magnetic field region and $z = -6''$ is practically outside the magnetic field of the magnet. Therefore, $\Delta L'_G(x)$ in inches was given by

$$\Delta L'_G(x) = \left\{ \int_{-7}^{3} B(x, z) dz / \int_{-3}^{4} B(x, z) dz \right\} - 3, \quad (21)$$

where

$$\int_{-3}^{4} B(x, z) dz = \int_{-6}^{4} B(x, z) dz - \int_{-7}^{3} B(x, z) dz,$$

For the measurement of $\Delta L'_G(x)$, we moved the search coil radially at 3" and 4". By keeping the radial displacement Δx constant ($\Delta x = 0.200''$), the gradient length in inches $\Delta L'_G(x)$ was given by

$$\Delta L'_G(x) = \frac{\int_{-7}^{3} B(x + \frac{\Delta x}{2}, z) dz - \int_{-7}^{3} B(x - \frac{\Delta x}{2}, z) dz}{\int_{-3}^{4} B(x + \frac{\Delta x}{2}, z) dz - \int_{-3}^{4} B(x - \frac{\Delta x}{2}, z) dz} - 3, \quad (22)$$

Figs. 5 and 6 give the distributions of $L'_B(x)$ and $L'_G(x)$ with final hard packs for both magnets. The designed usable regions at the hard packs, which is narrower on the outer side than that determined from the $X_0(x)$ distribution due to the shifting of the central orbit, are shown in these graphs. It can be seen that our requirements are well satisfied in these regions. These data were taken at 7.5 and 15 Gev excitation. We observed a slight saturation effect at the hard packs in L'_B and L'_G , which starts at 10 Gev. L'_B and L'_G shrink in by 13 mils with a wide gap magnet and 50 mils with a narrow gap magnet at 15 Gev. Distributions seem unaffected. This effect is due to the side surface of the hard packs which stick out of the surface of the coil. Therefore the narrow gap magnet shows a bigger effect (i.e. about 0.1% in L_B and L_G at 15 Gev). Also in Fig. 6 is shown $L'_G(x)$ of the uncorrected original hard pack.

Table II: Measured L_B and L_G at the center at 7.5 Gev

Magnet	L_{G0}	L_B	L_G	$L_B - L_G$
Wide Gap	126.48"	127.21" \pm .02"	125.99" \pm .04"	1.22"
Narrow Gap	126.48"	127.17" \pm .02"	126.09" \pm .04"	1.08"

In Table II is given the values of L_B and L_G at 7.5 Gev with their estimated errors of the measurement for both types of magnets.

Actually there are apparently bigger errors due to manufacturing. The errors in L_B and L_G due to this is estimated to be ± 40 mils and ± 110 mils respectively. The thermal expansion of the magnet is of the order of 2 mil/C for the temperature change of the cooling water.

The final shapes of the hard packs are shown in Fig. 7 and 8. Both sides of the pole pieces are tapered to accept the inside corners of the coils. The inclination of the pole pieces are punched out successively by a die which has two circular shapes of 1" radius connected with a straight line tangentially. The same die is used for both types of hard packs. To keep the same magnetic length and to use the same lamination stacking length in both types of magnets it was necessary to cut back the inclination of the hard packs of the wide gap magnet by about 0.36 inches more than for the narrow gap magnet.

52-266

The fringing fields with the final hard packs were measured at 2.5 kG AC excitation by the same technique as used before with two small search coils. The curves are shown in Fig. 9 and 10. The gradients of the fringing fields were obtained by taking the difference between two adjacent points in the radial direction. Figs. 11 and 12 show the gradients for both magnets. They show clearly how the field and gradient distributions are changed to meet our requirements.

References

1. P. N. Bredesen and P. C. Stein, CSDS-24, October 11, 1965
2. D. A. Edwards, CSDS 25 in press.
3. H. Nysater, CEA-29, April 16, 1957

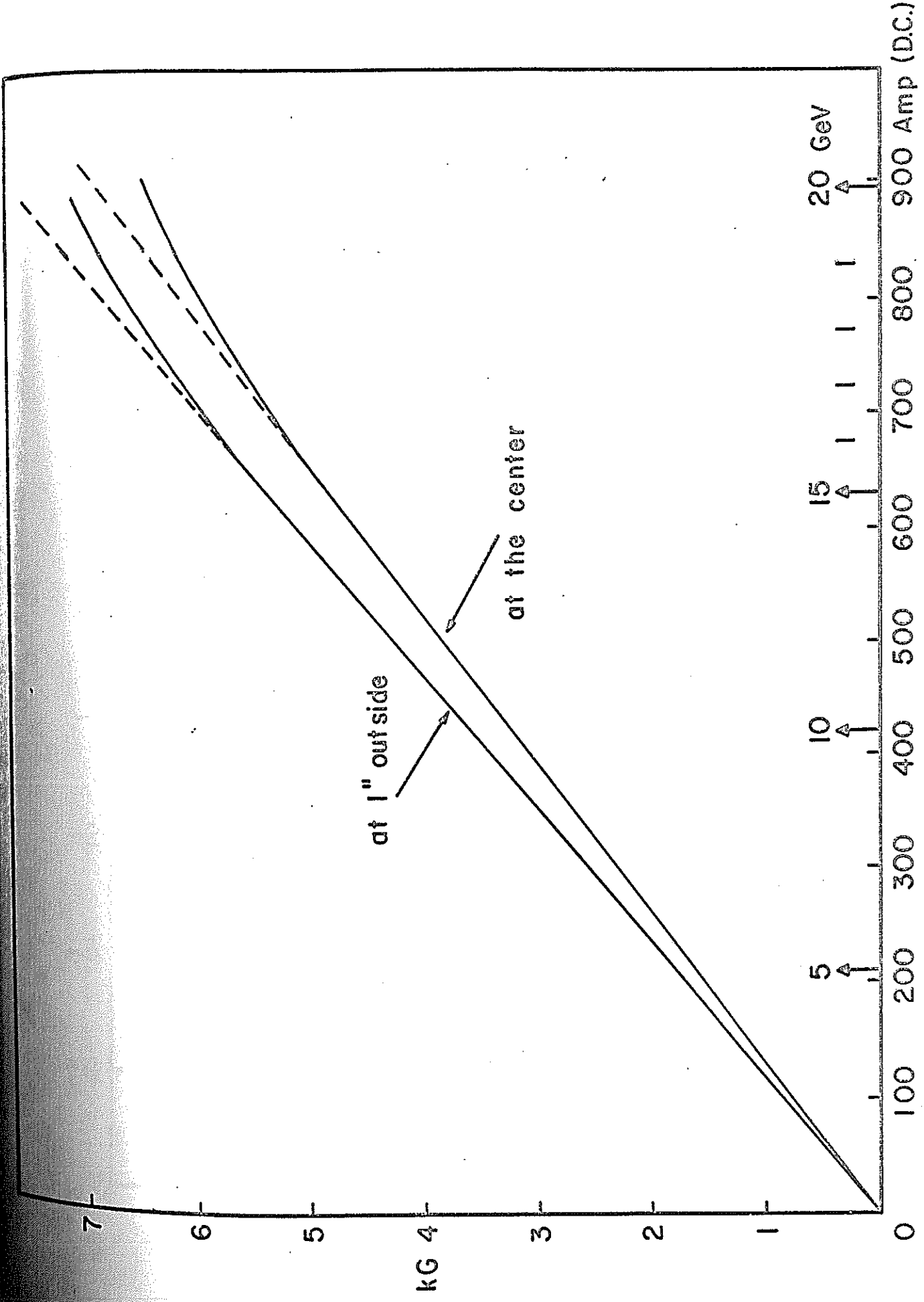


Fig. 1 Excitation Curve of Narrow Gap Magnet

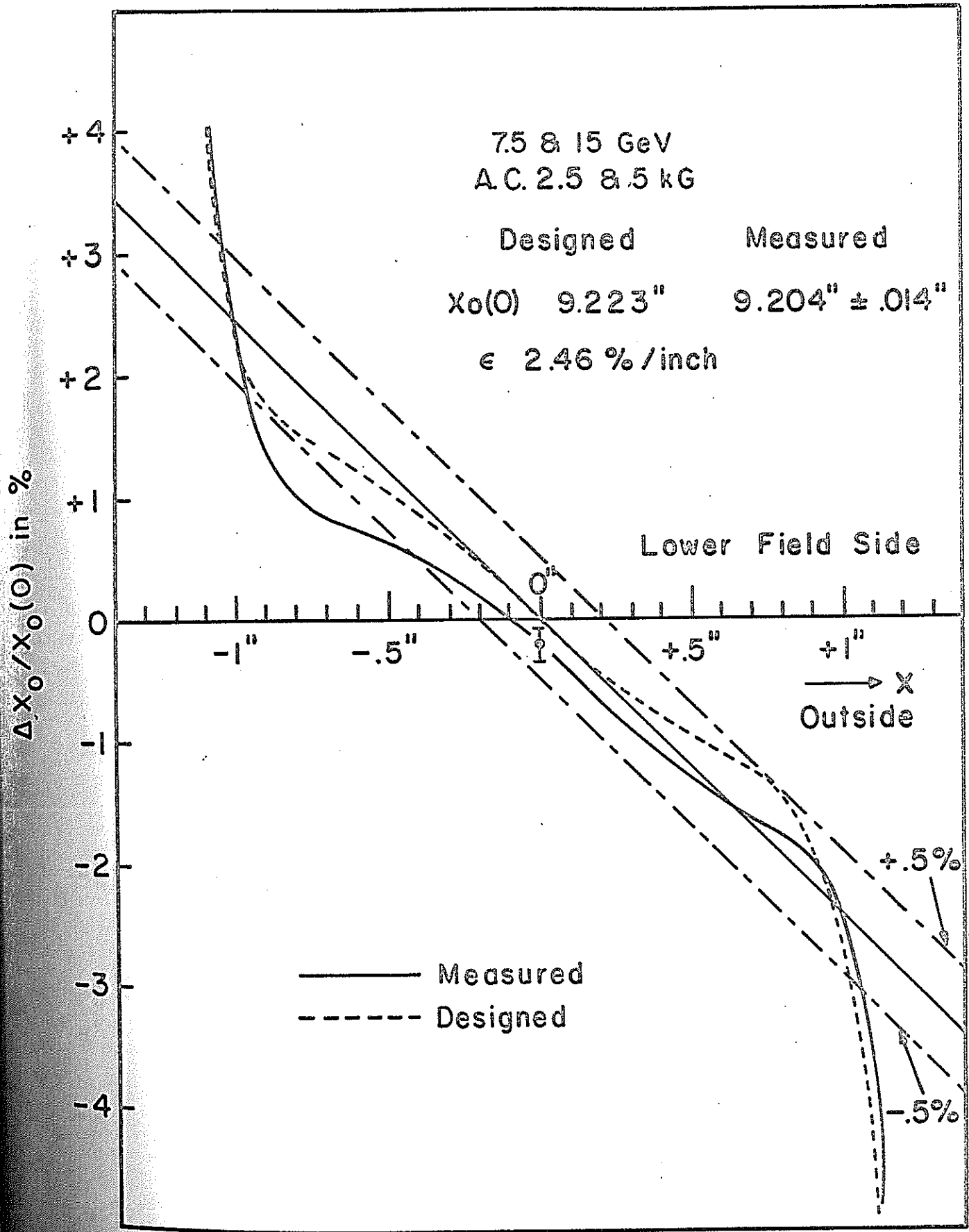


Fig.3 $X_0(x)$ Distribution of Wide Gap Magnet

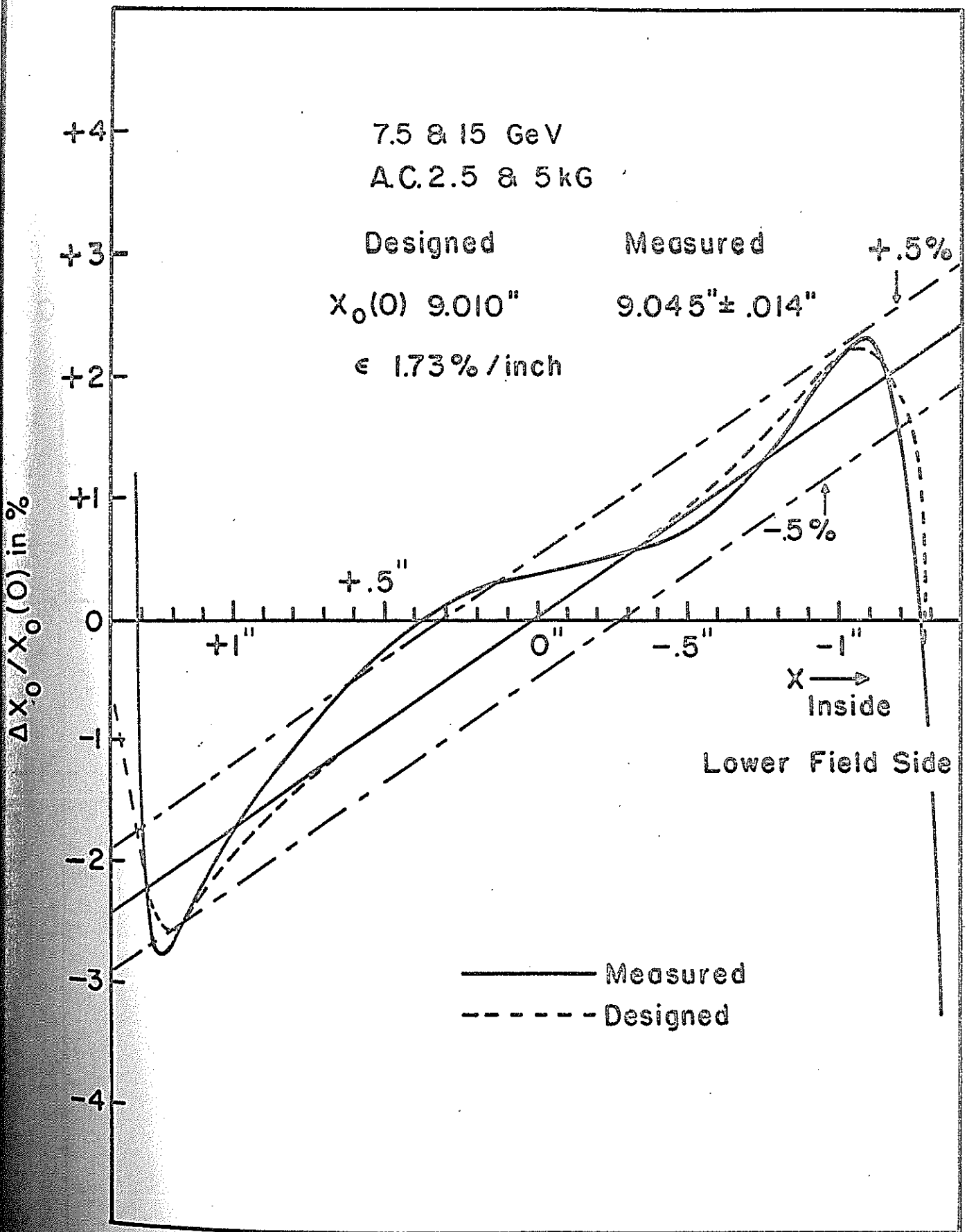


Fig.4 $X_0(x)$ Distribution of Narrow Gap Magnet

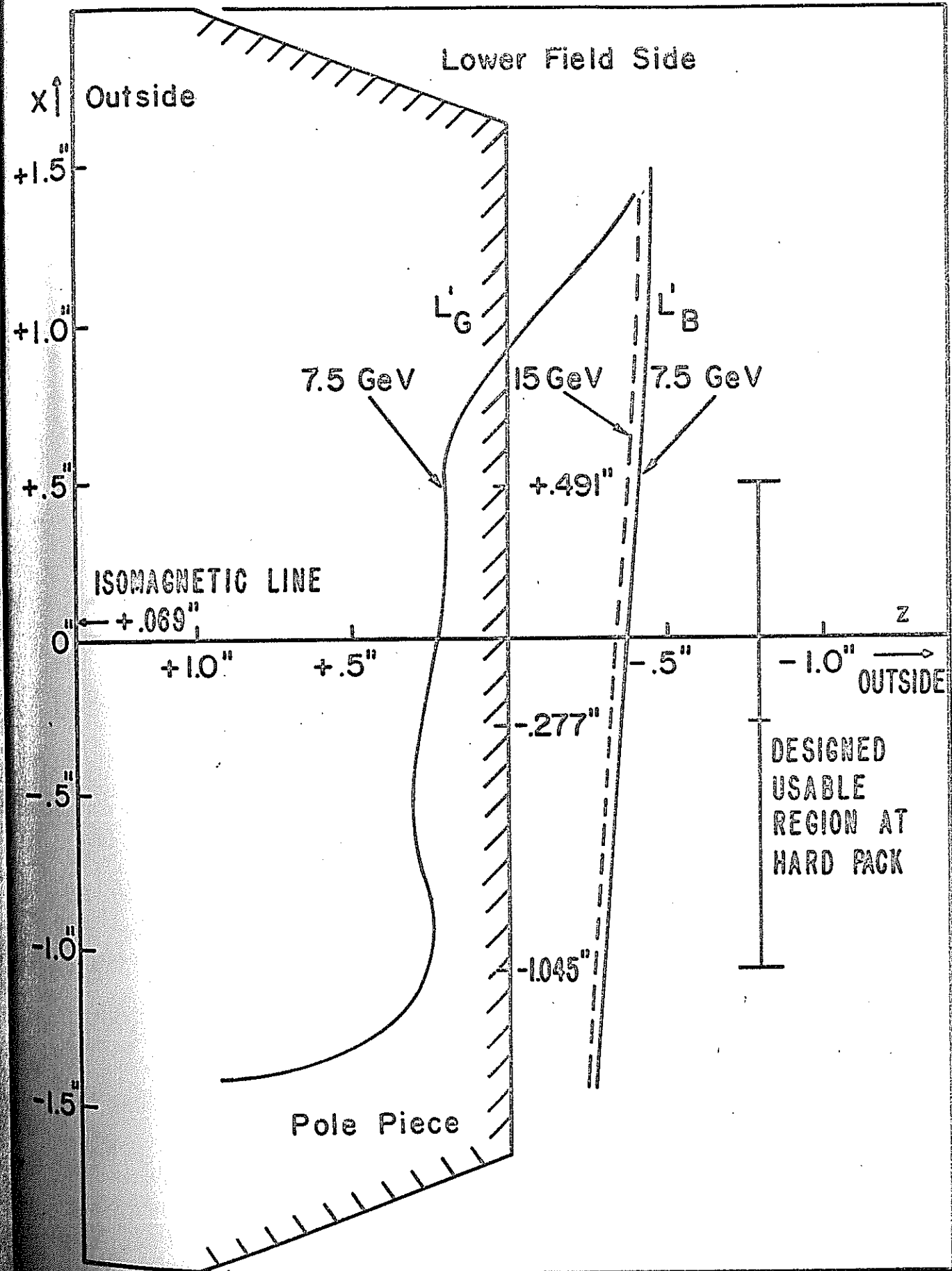


Fig.5 L'_B and L'_G of Wide Gap Magnet

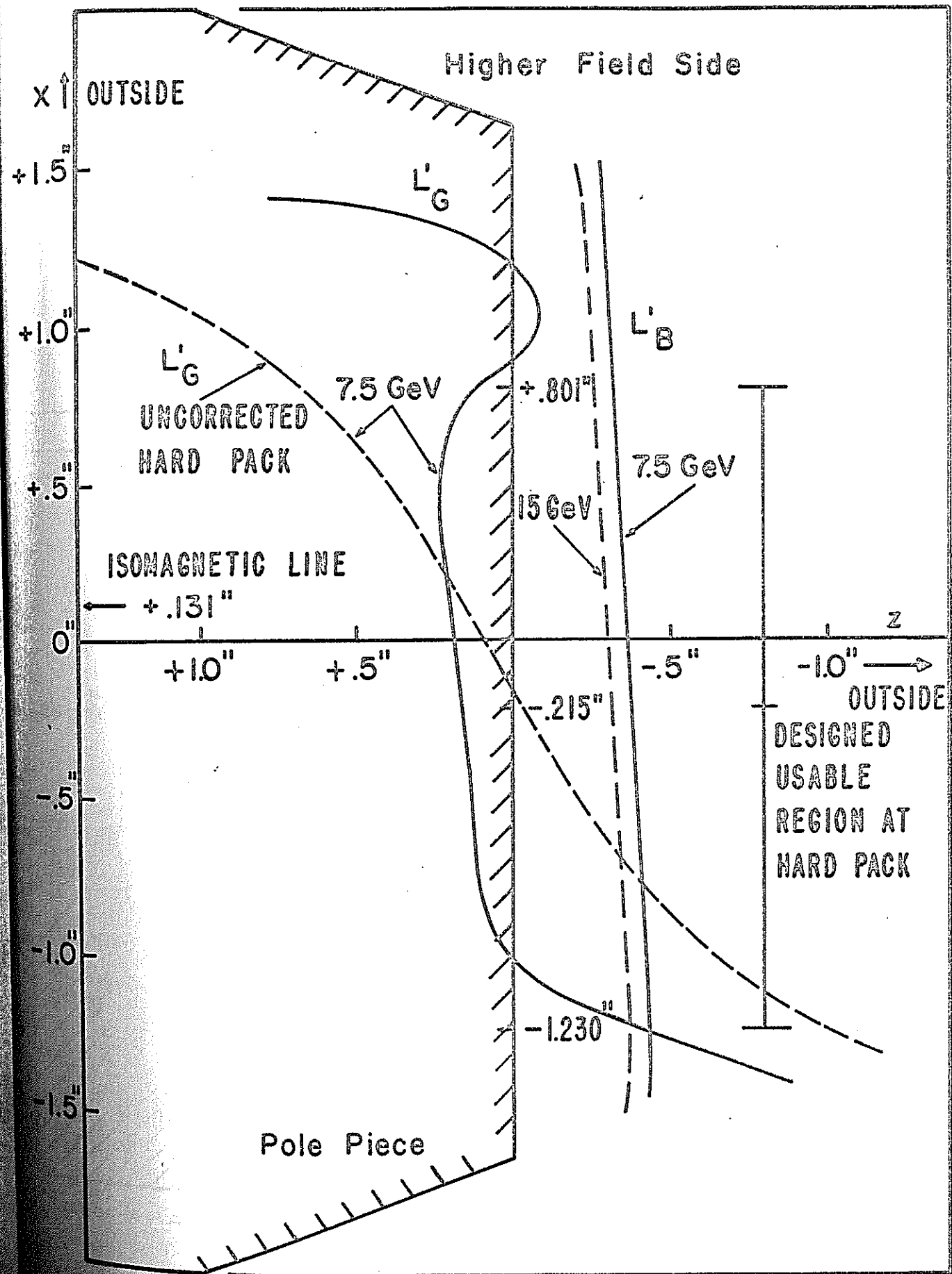
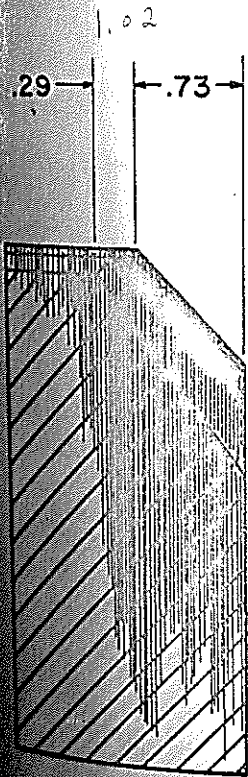
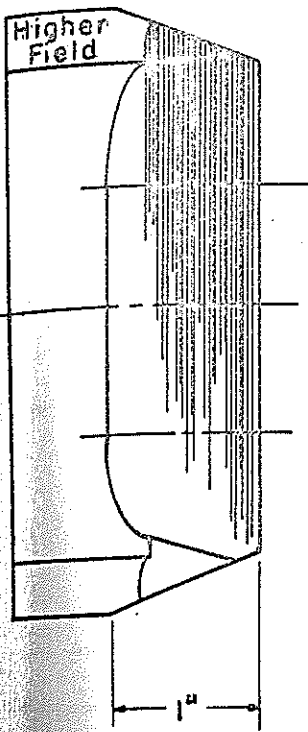


Fig.6 L'_B and L'_G of Narrow Gap Magnet



Section A-A

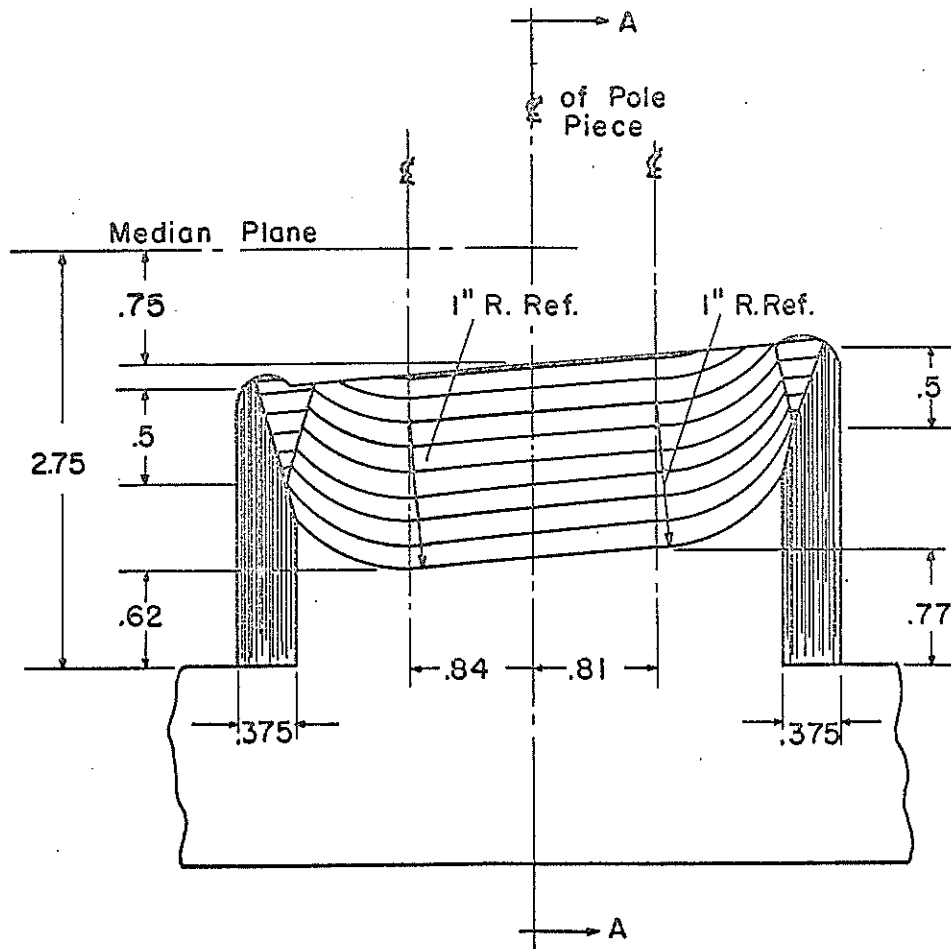


Fig. 7 Hard Pack of Wide Gap Magnet

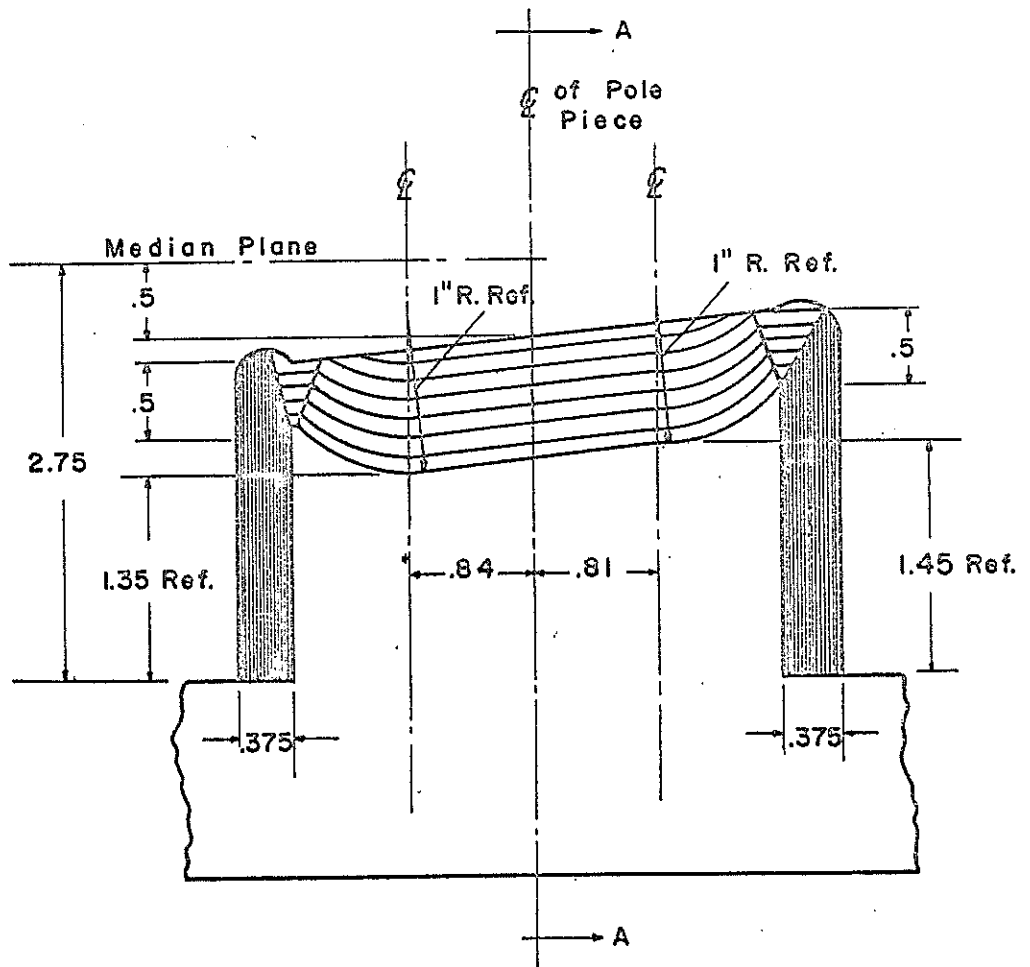
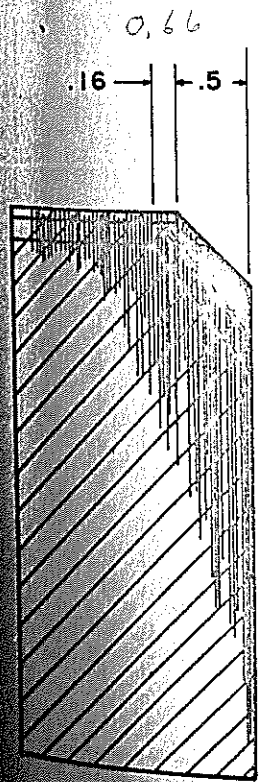
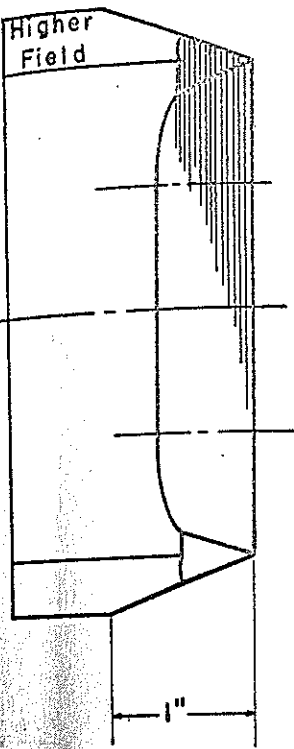


Fig 8 Hard Pack of Narrow Gap Magnet

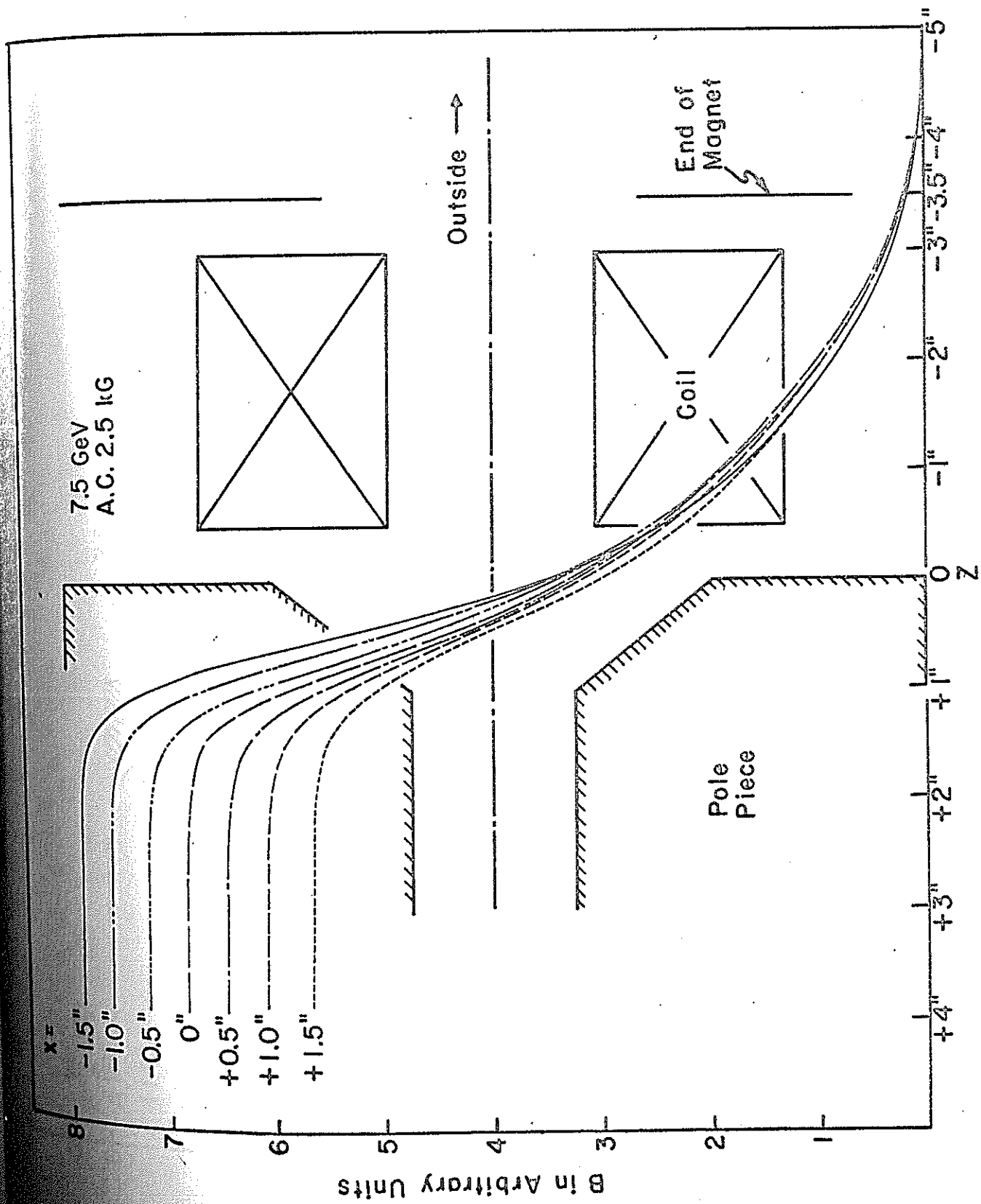


Fig. 9 Fringing Field of Wide Gap Magnet

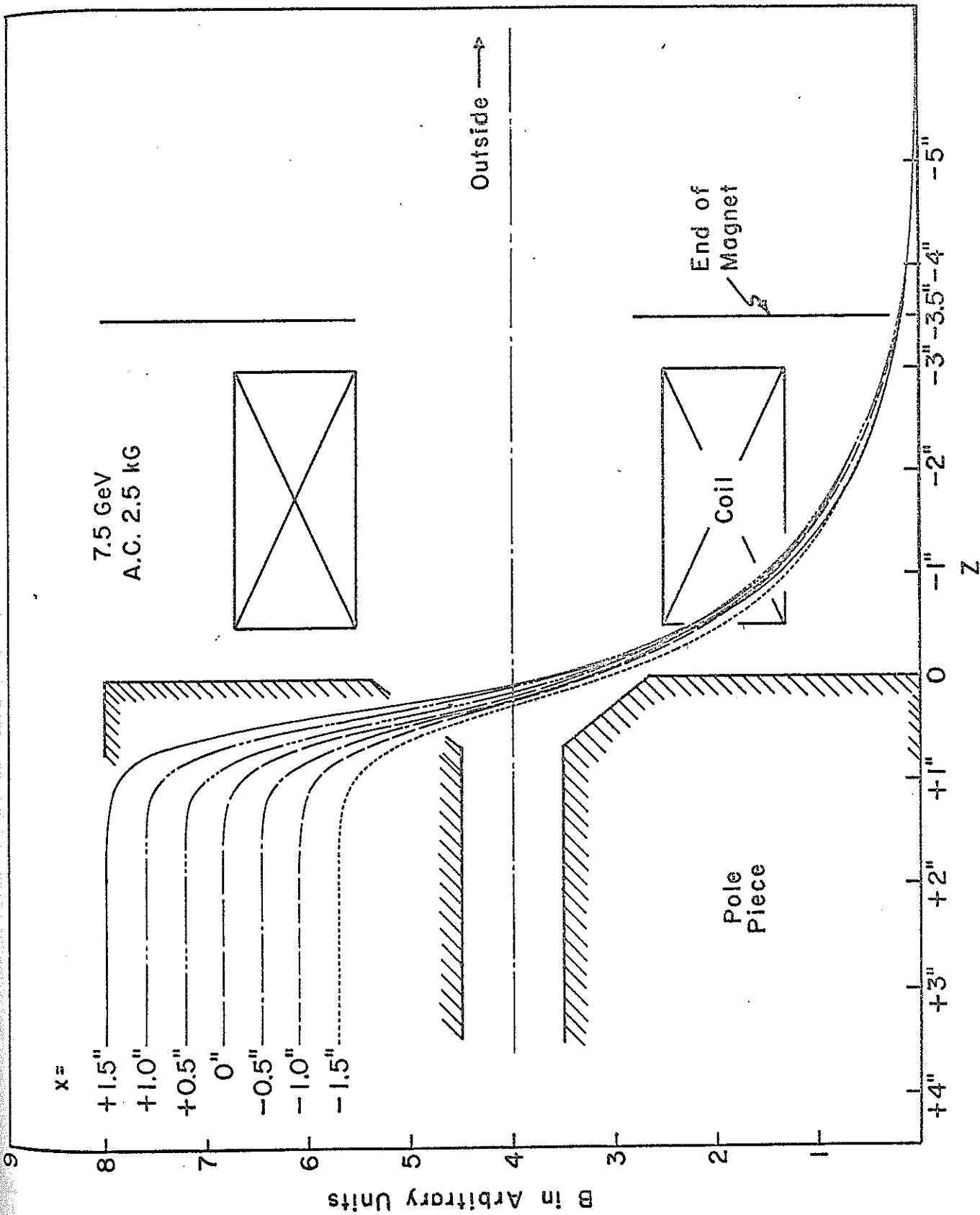


Fig. 10 Fringing Field of Narrow Gap Magnet

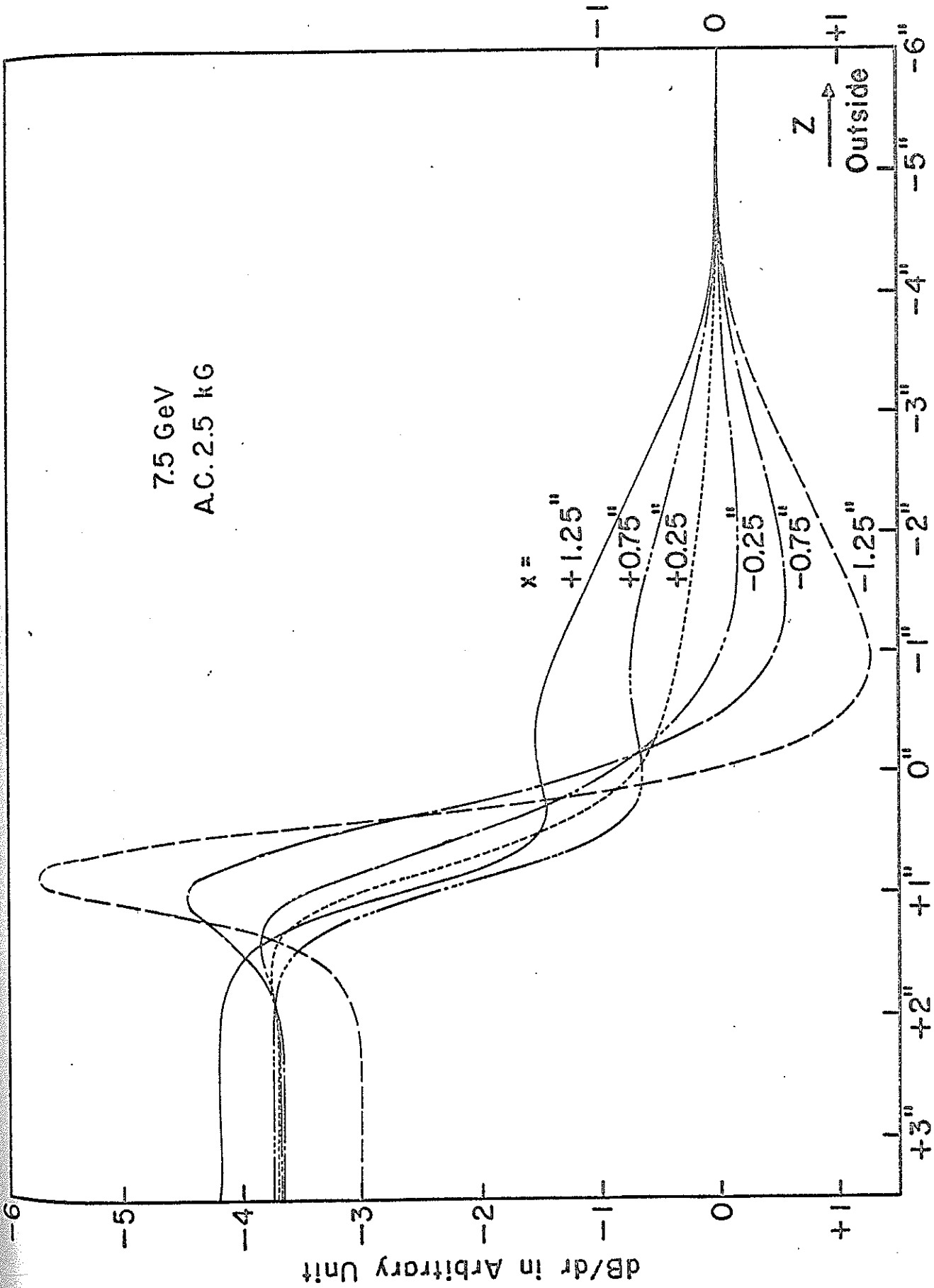


Fig.11 Gradient of Fringing Field of Wide Gap Magnet

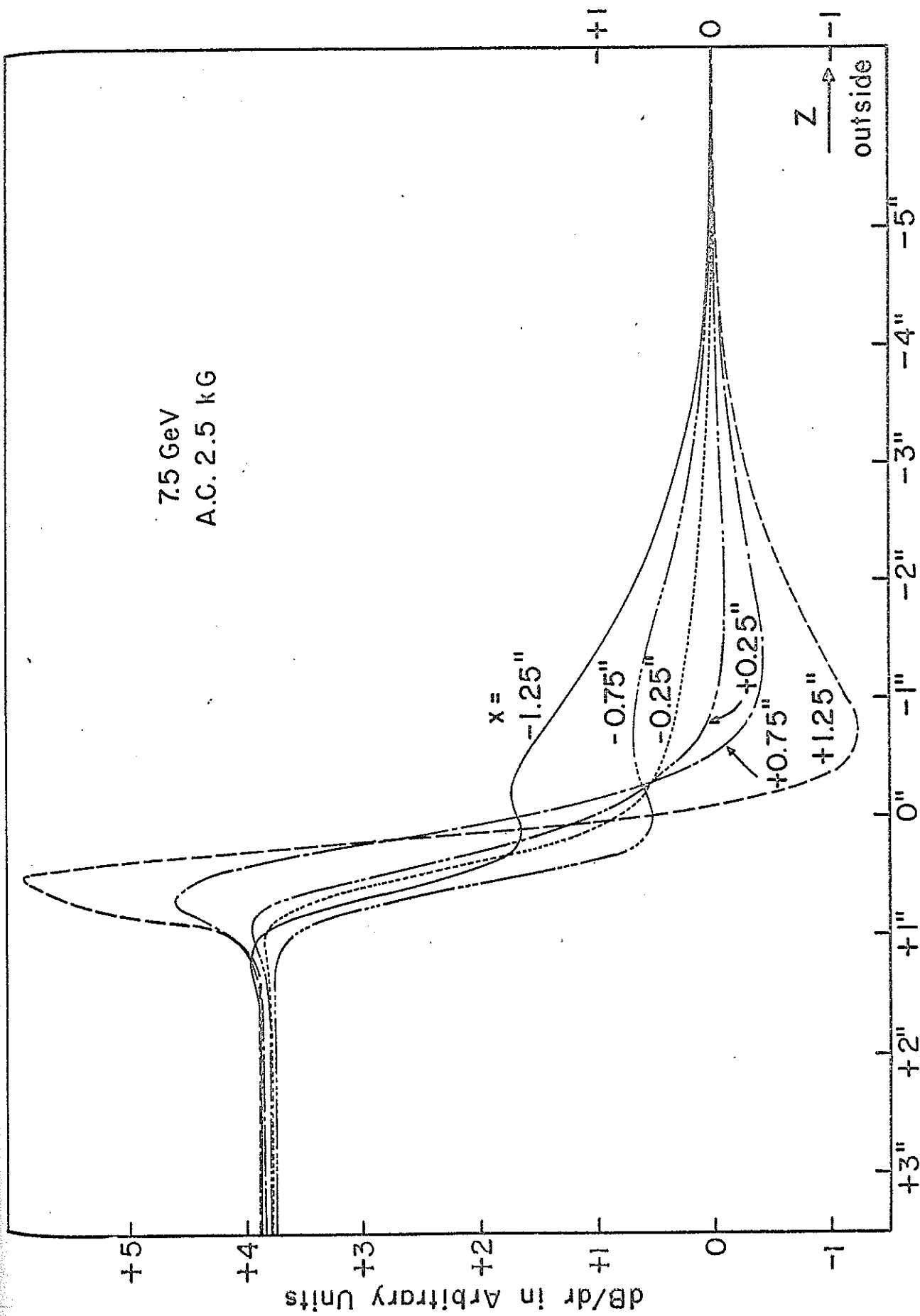


Fig.12 Gradient of Fringing Field of Narrow Gap Magnet